Biosensors and Bioelectronics 136 (2019) 84–90

Contents lists available at ScienceDirect

Biosensors and Bioelectronics

journal homepage: www.elsevier.com/locate/bios

Label-free microfluidic paper-based electrochemical aptasensor for ultrasensitive and simultaneous multiplexed detection of cancer biomarkers

Yang Wang[a,b], Jinping Luo[a,b], Juntao Liu[a,b], Shuai Sun[a,b], Ying Xiong[c], Yuanyuan Ma[c], Shi Yan[c], Yue Yang[c], Huabing Yin[d], Xinxia Cai[a,b,*]

[a] State Key Laboratory of Transducer Technology, Institute of Electronics, Chinese Academy of Sciences, Beijing, 100190, China
[b] University of Chinese Academy of Sciences, Beijing, 10090, China
[c] Key Laboratory of Carcinogenesis and Translational Research (Ministry of Education), Department of Thoracic Surgery II, Peking University Cancer Hospital & Institute, Beijing, 100142, China
[d] Division of Biomedical Engineering, School of Engineering, University of Glasgow, Oakfield Avenue, Glasgow, G12 8LT, United Kingdom

ARTICLE INFO

Keywords:
Electrochemical aptasensor
Microfluidic paper-based device
Nanocomposites
Multiplexed detection
Cancer biomarkers

ABSTRACT

Simultaneous detection of multiple tumor biomarkers in body fluids could facilitate early diagnosis of lung cancer, so as to provide scientific reference for clinical treatment. This paper depicted a multi-parameter paper-based electrochemical aptasensor for simultaneous detection of carcinoembryonic antigen (CEA) and neuron-specific enolase (NSE) in a clinical sample with high sensitivity and specificity. The paper-based device was fabricated through wax printing and screen-printing, which enabled functions of sample filtration and sample auto injection. Amino functional graphene (NG)-Thionin (THI)- gold nanoparticles (AuNPs) and Prussian blue (PB)- poly (3,4- ethylenedioxythiophene) (PEDOT)- AuNPs nanocomposites were synthesized respectively. They were used to modify the working electrodes not only for promoting the electron transfer rate, but also for immobilization of the CEA and NSE aptamers. A label-free electrochemical method was adopted, enabling a rapid simple point-of-care testing. Experimental results showed that the proposed multi-parameter aptasensor exhibited good linearity in ranges of 0.01–500 ng mL^{-1} for CEA (R^2 = 0.989) and 0.05–500 ng mL^{-1} for NSE (R^2 = 0.944), respectively. The limit of detection (LOD) was 2 pg mL^{-1} for CEA and 10 pg mL^{-1} for NSE. In addition, the device was evaluated using clinical serum samples and received a good correlation with large electrochemical luminescence (ECL) equipment, which would offer a new platform for early cancer diagnostics, especially in those resource-limit areas.

1. Introduction

With the increasingly worsening air pollution over the past decades, lung cancer has been one of the most threatening cancer to people's health and life worldwide (Lin et al., 2017; Song et al., 2016). The rapid simultaneous detection of multiple cancer biomarkers in body fluids could help confirm lung cancer as soon as possible, so as to provide scientific reference for clinical treatment (Xu et al., 2017). However, the determination of a single tumor marker usually has a limiting clinical reference value (Gao et al., 2017; Lu et al., 2015). Thus, simultaneous detection of two or more biomarkers, with high sensitivity and specificity, has gained lots of attention recently (Jia et al., 2014).

To date, immunoassay is one of the most widely accepted methods for detection of trace cancer biomarkers due to that antibody has high affinity towards the corresponding antigen (Zhang et al., 2008); (Mazzu-Nascimento et al., 2017). Various immunoassay technologies have been developed based on antibody-antigen interaction, including but not limited to radioimmunoassay (RIA) (Bast Jr et al., 1983), chemiluminescence immunoassay (CLIA) (Ge et al., 2012; Zong et al., 2012), fluorescence immunoassay (FIA) (Wacker and Niemeyer, 2004), electrochemiluminescence (ECL) (Babamiri et al., 2018), enzyme-linked immunosorbent assay (ELISA) (Gordon and Cross, 1990) and electrochemical immunoassay (EIA) (Lai et al., 2009; Tsai et al., 2016). Of all these above-mentioned methods, the label-free electrochemical method, for its outstanding advantages of high selectivity and sensitivity, has been recognized as a powerful tool for multiplexed detection of cancer biomarkers (Sun and Ma, 2013; Wei et al., 2018). In addition, it eliminates the need for labelling, making the detection a point-of-care testing. Some works based on electrochemical detection of single tumor marker have been reported before. For example, *Lv* et al. proposed a

* Corresponding author. State Key Laboratory of Transducer Technology, Institute of Electronics, Chinese Academy of Sciences, Beijing, 100190, China.
E-mail address: xxcai@mail.ie.ac.cn (X. Cai).

https://doi.org/10.1016/j.bios.2019.04.032
Received 21 February 2019; Received in revised form 12 April 2019; Accepted 16 April 2019
Available online 18 April 2019
0956-5663/

sandwich-type electrochemical immunosensor using AuNPs functionalized polydopamine (PDA) as transducing materials for detection of CEA, with a limit of detection of 0.167 pg mL^{-1} (Lv et al., 2018). *Zhang* et al. reported an electrochemical immunosensor, which employed reduced graphene oxide-thionin-hemin-Au (H-rGO-THI-Au) nanohybrid as probe, for highly sensitive measurement of NSE (Zhang et al., 2018).

However, compared to antibodies, nucleic acid aptamers have lower immunogenicity, higher affinity, wider receptor range and better selectivity, and thus have found increasing applications in scientific and industrial communities since its discovery (Hermann and Patel, 2000) (Famulok et al., 2000); (Song et al., 2008). The aptamers are generally selected by a mature technology called Systematic Evolution of Ligands by Exponential Enrichment (SELEX) (Fang and Tan, 2009), making them rather cost effective and chemically stable (Sefah et al., 2010). What's more, they offer remarkable flexibility for the structural design and easy modification of functional groups on their 5′ end (Gubala et al., 2011). Thus, aptamers have become increasingly important molecular tools in the field of diagnostics and therapeutics, leading to a range of aptamer receptors based bioassays (Maehashi et al., 2007; Zhou et al., 2014). In addition, not only the performance of the aptasensors has been significantly improved via the use of novel nanomaterials, but also the continuous development of nanotechnology offers a new horizon for aptamer-based detections (Sanghavi et al., 2015); (Wu et al., 2014).

Microfluidic paper-based device (μPAD), as an alternative platform for point-of-care testing, has gained tremendous attention since it was first reported by Whiteside's group (Martinez et al., 2007). After that, Henry's group has successfully introduced the electrochemical methods onto a paper device for the detection of glucose, lactate and uric acid by oxidase-based enzymatic reactions (Dungchai et al., 2009). In our previous work, a microfluidic paper-based electrochemical immunosensor modified with graphene nanocomposites was fabricated for highly sensitive and fast detection of CEA (Wang et al., 2016). Once the microfluidic channels were fabricated on μPAD, the flow direction of the liquid could be controlled, thus enabling simultaneous detection of multiple targets in a single biological sample. With so many attractive properties, such as low-cost, easy-to-use and portable, μPAD has become a promising and ideal analytical platform, especially in those less developed countries (Zhao et al., 2013); (Martinez et al., 2009).

In this paper, a paper-based device was fabricated for simultaneous multiplexed detection of CEA and NSE. The device could enable detection of two cancer biomarkers in a single biological sample. NG-THI-AuNPs and PEDOT-PB-AuNPs nanocomposites were synthesized and modified directionally onto the surface of the corresponding working electrodes, which could not only facilitate electron transfer capability but also increase the amount of immobilized aptamers, thus significantly enhancing the sensitivity of the electrochemical aptasensor. Adopting a label-free electrochemical detection method, the device could be used for point-of-care testing. This newly developed paper-based aptasensor, with high sensitivity, high selectivity and affordable diagnostic test device, would offer a new platform for early cancer diagnostic, especially in those resource-limit areas.

2. Experimental

2.1. Apparatus

Electrochemical measurements were performed with a Bio-Logic VMP3 multi-channel potentiostat (BIO-LOGIC, France). A three electrode system was used during measurement and all potentials given in this work were referred to the screen-printed Ag|AgCl electrode. To fabricate the microfluidic channels, a Xerox ColorQube 8570 digital wax printer was used to spray wax on the surface of paper, followed with baking in a Yiheng oven (DHG-9023A, Yiheng, China). Transmission electron microscopy (TEM) images of the nanocomposites were characterized on a Hitachi H7650 (HITACHI, Japan) transmission electron microscope.

2.2. Materials

DNA aptamer against CEA: 5′-ATA CCA GCT TAT TCA ATT-3' (Mw 5628.83 g mol^{-1}) and DNA aptamer against NSE: 5′-CGG TAA TAC GGT TAT CCA CAG AAT CAG GGG-3' (Mw 9476.29 g mol^{-1}) were synthesized and purified by Sangon Biotechnology Co. Ltd. (Shanghai, China). The two aptamers were modified with thiol groups on their 5′ end in order to bond with AuNPs. CEA and NSE antigens, Tris-Ethylenediaminetetraacetic acid (EDTA) buffer solution (10 mM Tris-HCl + 1 mM EDTA, pH = 8.0) were also obtained from Sangon Biotechnology Co. Ltd. $FeCl_3 \cdot 6H_2O$, $K_3[Fe(CN)_6]$ and HCl were purchased from Beijing Chemical Reagents Co. Ltd. (Beijing, China). Whatman NO. 1 chromatography paper was purchased from GE Healthcare Worldwide (Shanghai, China). The conductive carbon ink for working electrode and counter electrode was bought from Acheson, and Ag|AgCl ink (CNC-01) was from Yingman Nanotechnology Company. Other reagents, including thionine acetate was purchased from Alfa Aesar, 3,4-ethylenedioxythiophene (EDOT) and 6-mercaptohexanol (MCH) from Sigma-Aldrich and NG from Xianfeng Nanomaterials Company. All reagents were of analytical grade and used without further purification. Clinical serum samples were provided by Peking University Cancer Hospital & Institute.

2.3. Fabrication of paper microfluidics

Scheme 1 illustrates the paper-based aptasensor for multiplexed detection. The device can detect two analytes in one sample simultaneously as two working electrodes were integrated onto a single device. The device was fabricated on four pieces of cropped cellulose filter papers, and thus had the filtering function. For the operation of the device, a sample was introduced from the sample inlet located on the side, flowed through the microchannel, and reached the location where the three-electrode system was screen printed. Multiplexing analysis of the device was realized since the capillary action guided the sample to the two independent working electrodes on the paper within hot wax printed channels, and then recognized by the corresponding DNA aptamers (Wang et al., 2018). The device combined low cost and ease of use with the sensitivity of electrochemical detection.

Without the need of any specialized facilities or a clean room, the device was fabricated through four steps. The first step is to design the structures using Adobe Illustrator CS5. The size of the device was designed to be 10.5 mm × 35.0 mm. The counter electrode and the reference electrode were grouped together in one layer to form a circle, while the working electrode was located directly below. Registration marks were designed on each layer to ensure the assembling accuracy.

A filter paper was then printed with hot wax using a Xerox digital wax printer according to the designed pattern, followed by heating at 120 °C for 5 min in an oven to melt the printed wax. Because of the porous structure of the paper, the wax would diffuse through it to form the same hydrophobic pattern on both sides. Subsequently, three electrodes were screen printed on the corresponding site, where the working electrode and the counter electrode were of conductive carbon ink, while the reference electrode was of Ag|AgCl ink. Finally the papers were integrated together using a double side tape into the device.

2.4. Synthesis of NG-THI-AuNPs nanocomposites

The process of synthesizing NG-THI-AuNPs nanocomposites was as follows: a total of 2 mg NG was mixed with 2 mL ultrapure water in a round bottom flask, followed by 30 min ultrasonic process to form a stable NG solution. After that, 2 mL of THI solution (2 mg mL^{-1}) was added to the above flask and then stirred vigorously for 24 h. THI molecules would non-covalently attach to the surface of NG due to the π-π stacking interactions between benzene rings. Remove the non-

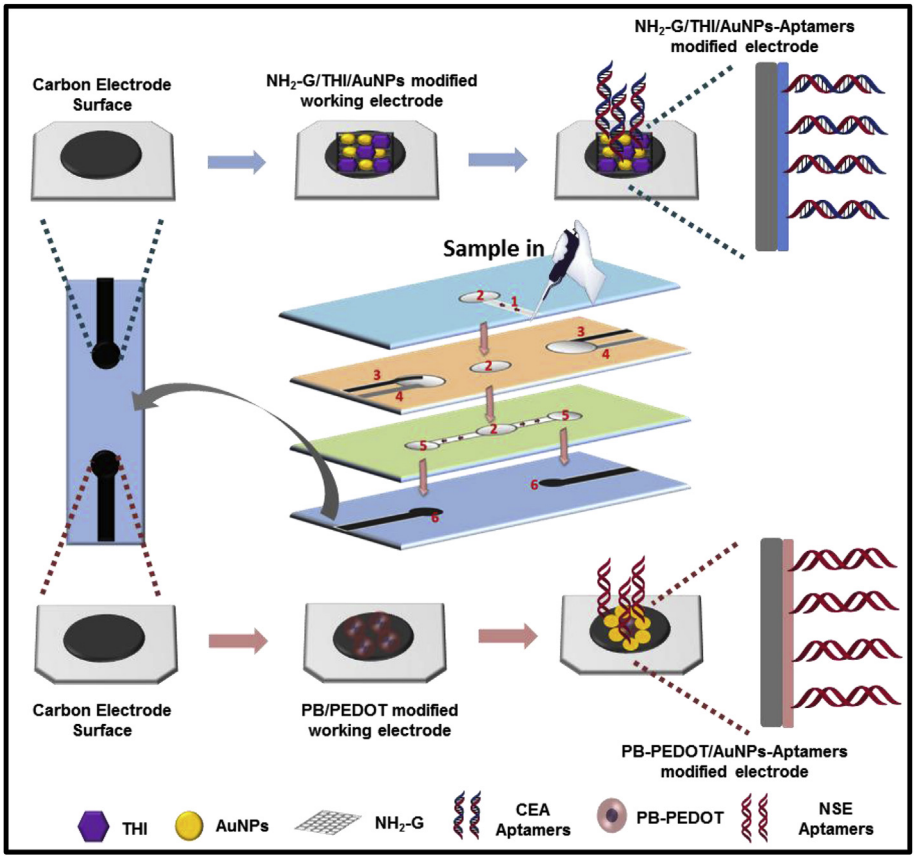

Scheme 1. Fabrication and modification process of the multi-parameter electrochemical paper-based aptasensor: (1) sample inlet hole; (2) filter hole; (3) screen-printed counter electrode; (4) screen-printed reference electrode; (5) detection zone; (6) screen-printed working electrode.

integrated THI molecules by centrifugation and washing several times to obtain the NG-THI nanocomposites. The as-synthesized nanocomposites were then dispersed in 2 mL water. Then 10 mL AuNPs solution, whose diameter was about 15 nm, was added to the above dispersion and stirred overnight to promote the AuNPs fully integration with the amino groups of NG. The AuNPs were prepared according to a literature (Guo and Wang, 2007). Finally, after washing and centrifugation, NG-THI-AuNPs nanocomposites were obtained and stored at 4 °C for further use.

2.5. Synthesis of PB-PEDOT-AuNPs nanocomposites

PB-PEDOT nanocomposites were synthesized by the oxidative polymerization of EDOT in the presence of Fe^{3+} ions (Yang et al., 2017). The specific reactions could be described as follows:

$$Fe^{3+} + EDOT \rightarrow Fe^{2+} + PEDOT \quad (1)$$

$$Fe^{2+} + [Fe(CN)_6]^{3-} \rightarrow Fe_3[Fe(CN)_6]_2\ (PB) \quad (2)$$

The two reactions above occurred in the same time in a typical synthesis. The PB-PEDOT nanocomposites were of core-shell structure, which could significantly improve the stability and conductivity of PB. Briefly, 50 μL EDOT was first dissolved in 5 mL of ethanol solution and then transferred to 25 mL of 0.1 M HCl to form a stable solution. Meanwhile, 13.2 mg $K_3[Fe(CN)_6]$ and 10.8 mg $FeCl_3{\cdot}6H_2O$ were added to 10 mL of 0.1M HCl solution and then sonicated for 30 min. The obtained two solutions were mixed together under vigorously stirring. As the reaction proceeded, the color of the mixture turned into dark blue gradually, indicating the formation of PB-PEDOT nanocomposites. After centrifugation and washing, the mixture was dried in an oven. Eventually, 10 mL of AuNPs solution was added to 2 mL PB-PEDOT suspension (1 mg mL^{-1}) and stirred overnight to form PB-PEDOT-AuNPs nanocomposites.

2.6. Fabrication of the multiplexed paper-based aptasensor

The schematic diagram of the stepwise modification process of the multiplexed paper-based aptasensor was also shown in Scheme 1. For the fabrication, 10 μL NG-THI-AuNPs and 10 μL PB-PEDOT-AuNPs nanocomposites were coated on the corresponding surface of working electrode of the microfluidic paper device, separately. Put the modified device at 50 °C in an oven for half an hour. Then 10 μL of CEA aptamers was dropped onto the surface of NG-THI-AuNPs modified electrode while another 10 μL of NSE aptamers was introduced onto the PB-PEDOT-AuNPs modified electrode, followed with washing with 1 mL of TE buffer (10 mM Tris-HCl, 1 mM EDTA, pH 7.4) to remove the unbound aptamers. The concentrations of CEA and NSE aptamers were optimized at 28 μg mL^{-1} and 47 μg mL^{-1}, respectively. As the aptamers had already been modified with thiol groups on their 5' end, which facilitated their conjugation with AuNPs through Au−S bond. Next, 10 μL of 1 mM MCH solutions were employed to block any nonspecific binding sites. After 1 h of incubation at room temperature, the modified paper aptasensor was washed with 1 mL of TE buffer three times. The prepared aptasensor was stored at 4 °C for further use. Each time before electrochemical measurement, 20 μL biological samples, such as standard solutions and clinical serum samples, containing certain concentration of CEA and NSE antigens were added to the device from the sample inlet hole and incubated for 1 h.

2.7. Electrochemical measurements of CEA and NSE

The basic electrochemical properties of the developed paper-based

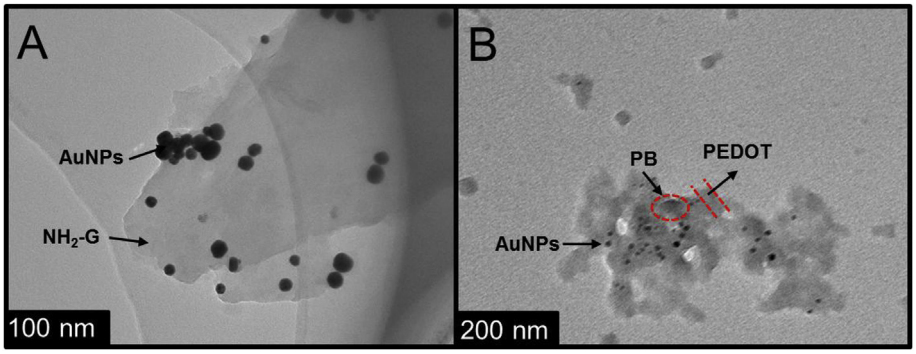

Fig. 1. TEM images of the synthesized nanocomposites. (A) TEM image of NG-THI-AuNPs nanocomposites; (B) TEM image of PB-PEDOT-AuNPs nanocomposites.

aptasensor were mainly characterized by cyclic voltammetry (CV) while the response to the CEA and NSE antigens were conducted by the differential pulse voltammetry (DPV). All electrochemical experiments were carried out in a VMP3 multi-channel potentiostat in PBS solution (pH = 7.4). The DPV curves were recorded in the range of −0.5 V to 0.3 V, with 5 mV step potential, 0.025 s modulation time and 0.5 s interval time. Besides, CV was conducted at a scan rate of 100 mV s^{-1} between −0.5 V and 0.3 V. Two sets of conventional three-electrode system were integrated into a single paper device.

3. Results and discussions

3.1. Characterization of NG-THI-AuNPs and PB-PEDOT-AuNPs nanocomposites

NG-THI-AuNPs and PB-PEDOT-AuNPs nanocomposites were synthesized to immobilize CEA and NSE aptamers, separately. TEM images (Fig. 1A–B) illustrated the morphology of the synthesized two nanocomposites. NG showed wrinkled paper-like structure (Fig. 1A), which could provide a large surface area to load the electrochemical-active thionin molecules through π-π stacking interactions. AuNPs, with a size of approximately 15 nm, were clearly observed on the surface of graphene. They were immobilized because of the interactions between gold and amino groups. The synthesized PB-PEDOT-AuNPs showed a 3D hierarchical porous structure (Fig. 1B), which could significantly improve the stability of the PB molecules. Their unique structure and large surface area, could promote the electron transfer rate, thus enhancing the current signal. In addition, the AuNPs were distributed uniformly within the matrix, which facilitated not only the electron transfer, but also immobilization of the thiol modified aptamers of CEA and NSE through Au−S bond.

3.2. Electrochemical characterization of the paper-based aptasensor

Electrochemical detection methods, including CV and DPV, were used to characterize basic properties of the paper-based electrochemical aptasensor after successful modification with NG-THI-AuNPs and PB-PEDOT-AuNPs nanocomposites. Fig. 2A and Fig. 2B showed the result of CV scan, which could be used to investigate the properties of electrode surface. Compared with bare working electrode, well behaved electrochemical responses which exhibited two pronounced redox peaks were obtained due to the electroactivity of THI and PB molecules (Jia et al., 2014; Sun et al., 2013). The redox couple at −0.19/-0.31 V was observed due to the electroactivity of THI molecules while the redox couple at +0.04/-0.07 V was due to PB molecules (Yu et al., 2013; Yang et al., 2017). As shown in Fig. 2A and B, the presence of two similar peaks, i.e. cathodic and anodic, was consistent with a typical reversible electrochemical behavior. In addition, the electrochemical performance of step-wise immobilization procedure of the aptasensor was also monitored in 0.1M PBS solutions. The current intensity decreased gradually when corresponding antigens were added onto the surface of the electrode, which was attributed to the fact that the formation of aptamer-antigen complex would inhibit the electron transfer process. Furthermore, with a higher concentration of antigen, more immunocomplex would form, thus resulting in a lower current intensity.

DPV responses of the aptasensor were shown in Fig. 2C. DPV is a well-established technique to measure the strength of electrical activity with a much higher sensitivity. Compared with bare working electrode (the blue line), the modified electrode showed two pronounced redox peaks at −0.22 V (the black line) and 0.01 V (the red line), and whose peak current was 18.02 μA and 14.06 μA, respectively. Subsequently, the peak current decreased then the corresponding electrode was immobilized with aptamer and antigen. The result of DPV measurements was highly consistent with the principle of our detection method. From the results above, we could conclude that the proposed multiplexed electrochemical aptasensor was successfully modified and could be used for simultaneous determination of CEA and NSE in a single sample.

3.3. Optimization of the size of AuNPs for the response of aptasensor

AuNPs have attracted a lot of attention due to their excellent conductivity and fascinating properties. They have been extensively used to develop a variety of highly sensitive biosensors, especially electrochemical biosensors. In this work, the AuNPs could not only promote electron transfer between the immobilized electroactive materials and the electrode surfaces, but also provide an ideal microenvironment for immobilization of CEA and NSE aptamers through the interaction between Au and the −SH modified on the 5′ end of the aptamers. Thus, it is crucial to choose an optimal size of AuNPs. Different sizes of AuNPs (5 nm, 10 nm, 15 nm, 25 nm, 50 nm, 100 nm) were prepared and used to modify the aptasensor. As shown in Fig. S2A, the current response of DPV reached maximum at 15 nm. What's more, TEM images of the synthesized AuNPs were observed to further investigate the size. As shown in Fig. S2B, the diameters of the AuNPs were about 15 nm. As a result, AuNPs of 15 nm were used in the following experiments.

3.4. Simultaneous multiplexed detection of CEA and NSE by the aptasensor

Under optimal conditions, the sensitivity and dynamic range of the multiplexed detection aptasensor for CEA and NSE were tested by measuring the change in peak currents of DPV responses. Each aptasensor was incubated with a single biological sample which contained certain concentrations of CEA and NSE before measurement. The detection of the two analytes was based on the degree of decreased peak currents of DPV responses, which was attributed to the formation of aptamer-antigen complex on the surface of the electrode. As shown in Fig. 3, with the increasing of CEA (Fig. 3A) and NSE (Fig. 3C), the currents decreased gradually. The calibration plots displayed a good

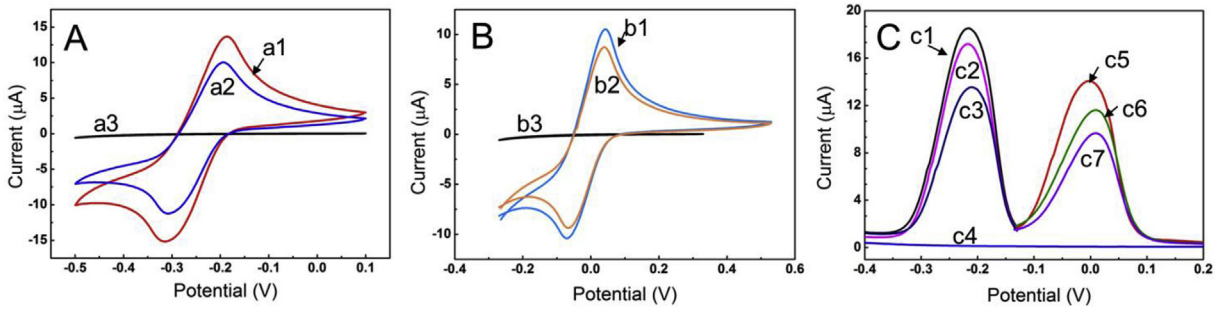

Fig. 2. Electrochemical properties of the paper-based aptasensor monitored in 0.1 M PBS solution (pH = 7.4). (A) CV responses of the NG-THI-AuNPs modified working electrode for CEA detection: (a1) NG-THI-AuNPs nanocomposites modified electrode; (a2) NG-THI-AuNPs/CEA aptamer modified electrode; (a3) bare working electrode; (B) CV responses of the PB-PEDOT-AuNPs modified working electrode for NSE detection: (b1) PB-PEDOT-AuNPs nanocomposites modified electrode; (b2) PB-PEDOT-AuNPs/NSE aptamer modified electrode; (b3) bare working electrode; (C) DPV responses of the multi-parameter paper-based aptasensor towards CEA and NSE: (c1) NG-THI-AuNPs nanocomposites modified electrode; (c2) NG-THI-AuNPs/CEA aptamer modified electrode; (c3) the multi-parameter aptasensor incubated with 100 pg mL^{-1} of CEA; (c4) bare working electrode; (c5) PB-PEDOT-AuNPs nanocomposites modified electrode; (c6) PB-PEDOT-AuNPs/NSE aptamer modified electrode; (c7) the multi-parameter aptasensor incubated with 100 pg mL^{-1} of NSE.

linear detection relationship between the peak currents and the concentration of analytes in the ranges of 0.01–500 ng mL^{-1} for CEA (R^2 = 0.989) and 0.05–500 ng mL^{-1} for NSE (R^2 = 0.944), respectively. In addition, the regression equation obtained between the peak currents of DPV and logarithm concentration of analytes was I_{dpv} (μA) = 18.495 − 2.796 lg C_{CEA} (ng mL^{-1}) for CEA and I_{dpv} (μA) = 11.092 − 1.444 lg C_{NSE} (ng mL^{-1}) for NSE, separately. The limit of detection (LOD), calculated by the 3σ/S where σ is the standard deviation of the lowest signal and S is the slope of linear calibration plot, was 2 pg mL^{-1} for CEA and 10 pg mL^{-1} for NSE, respectively.

Many studies for quantitative detection of CEA and NSE were based on various methods and different platforms. The comparison between the proposed aptasensor and some typical biosensors were shown in Table S1. The result illustrated that our paper-based aptasensor had a relatively wide linear range and a reasonable low detection limit. What's more, typically in clinical practice, a level of 5 ng mL^{-1} for CEA and 15 ng mL^{-1} for NSE in human serum sample are considered as the cut-off value for potential diagnosis of lung cancer. Thus, the multiplexed detection paper-based aptasensor fabricated in this work could provide an alternative platform for the early diagnosis of lung cancer.

3.5. Repeatability, stability and selectivity of the paper-based aptasensor

The selectivity and specificity of biosensors are of crucial importance for its clinical application with clinical serum samples. To characterize the specificity, 1 ng mL^{-1} of CEA and NSE was separately mixed with 10 ng mL^{-1} of some potential interference, including Bovine Serum Albumin (BSA), Uric Acid (UA), Ascorbic Acid (AA) and Cyfra21-1. As shown in Fig. 4A and Fig. 4B, although the added concentration of interference were 10 times higher than that of target CEA or NSE molecules, the variation in current was less than 6.22%. What's more, the selectivity of the proposed aptasensor was also studied through the comparison of the peak currents of 1 ng mL^{-1} CEA or NSE with 1 ng mL^{-1} of above-mentioned interference. All results indicated that the proposed multi-parameter had good specificity for both CEA and NSE.

For the low-cost disposable paper-based aptasensor, repeatability is an important parameter. Each fabricated paper-based device contained

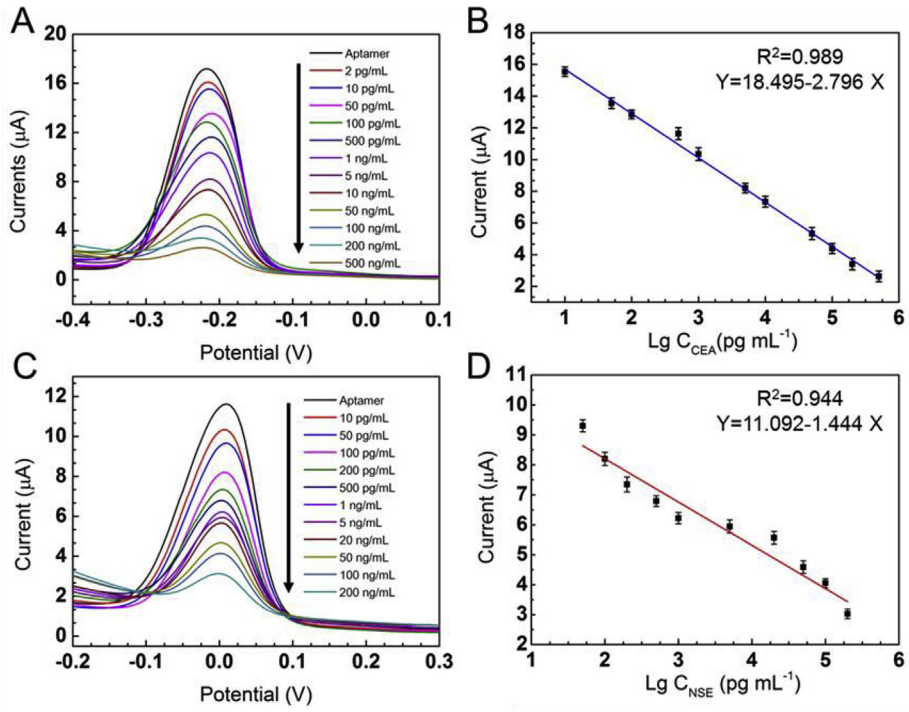

Fig. 3. Assay results of simultaneous multiplexed detection of CEA and NSE in 0.1M PBS solution (pH = 7.4). (A) DPV responses to different concentrations of CEA antigens; (B) The calibration curve between the peak current and logarithm concentration of CEA; (C) DPV responses to different concentrations of NSE antigens; (D) The calibration curve between the peak current and logarithm concentration of NSE.

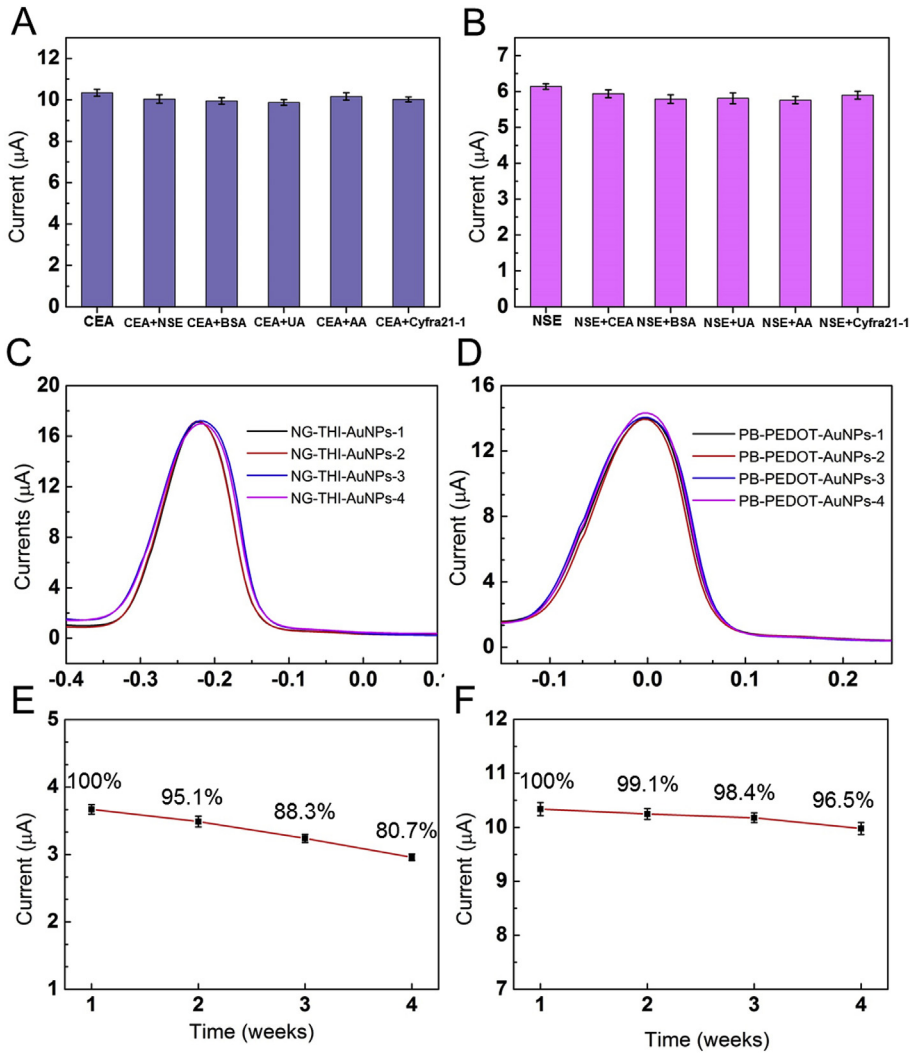

Fig. 4. Evaluation of basic properties of the proposed multi-parameter paper-based aptasensor. (A) Comparison of DPV response of the aptasensor to 1 ng mL^{-1} CEA and 1 ng mL^{-1} CEA mixed with 10 ng mL^{-1} NSE, BSA, UA, AA, Cyfra21-1, separately; (B) Comparison of DPV response of the aptasensor to 1 ng mL^{-1} NSE and 1 ng mL^{-1} NSE mixed with 10 ng mL^{-1} CEA, BSA, UA, AA, Cyfra21-1, separately; Repeatability results of (C) NG-THI-AuNPs/CEA aptamer modified electrode and (D) PB-PEDOT-AuNPs/NSE aptamer modified electrode; (E) Long-term storage stability of the former proposed paper-based immunosensor to 1 ng mL^{-1} CEA; (F) Long-term storage stability of the aptasensor to 1 ng mL^{-1} CEA.

two pairs of electrochemical cell (working electrode, counter electrode and reference electrode). To evaluate the repeatability of the multiplexed detection aptasensor, four different modified devices were scanned in 0.1M PBS solution by electrochemical workstation. As shown in Fig. 4C and D, the coefficient of variation was 0.56% for NG-THI-AuNPs-CEA aptamer modified electrode and 1.22% for PB-PEDOT-AuNPs-NSE aptamer modified one, indicating a good repeatability for the multiplexed detection.

Besides, the stability of the prepared aptasensor was evaluated by keeping the device at 4 °C and then scanned the electrode per week. As shown in Fig. 4E and F, the DPV response of the aptasensor to 1 ng mL^{-1} CEA could remain 96.5% of their origin response after four weeks of storage, while the paper-based immunosensor we fabricated before could only remain 80.7% of the response (Wang et al., 2016). The immunosensor was modified with NH_2-G/THI/AuNPs nanocomposites and adopted CEA antibody as the specific recognition element. As we know, the aptamers were selected and synthesized artificially, which were more stable and could be even stored at room temperature for a long time. Thus, with the same nanomaterials and a more stable recognition element, the responses of the new sensor to CEA were more stable. The results indicated that the sensor had the potential for long-term use.

3.6. Clinical validation with serum samples

To further validate the clinical application of our aptasensor, fifteen clinical serum samples provided by the Peking University Cancer Hospital were tested. All samples, which contained both CEA and NSE, had already been tested in the central lab of the hospital using a commercial-available Roche electrochemiluminescence apparatus. The clinical serum samples were detected directly with our sensor without any dilution and the analytical results were compared with the reference values provided by the hospital. As shown in Table .1, the relative errors between these two methodologies are less than 7.81% for CEA and 22.43% for NSE, indicating a good accuracy and high sensitivity for simultaneously detection of CEA and NSE in clinical serum samples.

4. Conclusion

In this work, a multi-parameter electrochemical paper-based aptasensor was designed and fabricated for the simultaneous detection of CEA and NSE in one clinical sample. The microfluidic channels of the paper device was fabricated by wax printing while the three-electrode system (working electrode, counter electrode and reference electrode) was made by screen printing. Nano composites were synthesized to modify the electrodes not only for the immobilization of CEA and NSE aptamers, but also for the signal amplification. Under optimal conditions, the multi-parameter aptasensor exhibited good linearity in ranges of 0.01–500 ng mL^{-1} for CEA (R^2 = 0.989) and 0.05–500 ng mL^{-1} for NSE (R^2 = 0.944), respectively. The limit of detection (LOD) calculated by the 3σ/S was 2 pg mL^{-1} for CEA and 10 pg mL^{-1} for NSE,

Table 1
Assay results of simultaneous detection of CEA and NSE in a same clinical serum sample.

No.	CEA			NSE		
	Measured C (ng mL^{-1})	Reference C (ng mL^{-1})	Relative Errors (%)	Measured C (ng mL^{-1})	Reference C (ng mL^{-1})	Relative Errors (%)
1	1.28	1.25	2.03	12.38	14.49	−14.59
2	1.46	1.49	−1.71	9.05	11.67	−22.43
3	2.09	1.97	6.28	13.53	15.64	−13.52
4	2.32	2.39	−3.13	15.82	14.63	8.15
5	2.77	2.89	−4.13	14.83	13.73	7.98
6	3.32	3.08	7.81	16.54	14.57	13.55
7	3.33	3.19	4.53	8.79	8.00	9.82
8	3.51	3.44	2.11	11.01	11.82	−6.86
9	5.17	4.82	7.33	20.56	19.12	7.52
10	5.86	5.51	6.34	14.43	15.71	−8.13
11	6.19	6.69	−7.53	13.80	12.27	12.48
12	7.57	7.83	−3.26	15.59	17.34	−10.09
13	9.83	9.20	6.83	16.81	18.42	−8.76
14	9.88	10.18	−2.95	22.70	19.67	15.39
15	15.54	16.12	−3.61	16.47	15.02	9.68

respectively. In summary, there are three key benefits of the proposed multi-parameter aptasensor: (1) the aptasensor contained two working electrodes, which could enable simultaneous detection of two tumor markers in a single sample with high sensitivity and selectivity, so as to provide scientific guidance reference for clinical treatment; (2) the aptasensor had a fast response time as a label-free electrochemical detection method, which provides a powerful tool for the point-of-care testing of cancer biomarkers; (3) the aptasensor was made on paper by wax printing and screen-printing, which could be mass-produced easily with low cost. In addition, the cost of a paper device was calculated roughly and the total expense was about $ 0.12. This would greatly expand its application to those less developed countries. As a result, the proposed aptasensor could provide an optional low-cost and portable diagnostics platform for the cancer biomarkers.

CRediT authorship contribution statement

Yang Wang: Writing - original draft, Writing - review & editing, Methodology, Formal analysis. **Jinping Luo:** Investigation. **Juntao Liu:** Investigation. **Shuai Sun:** Validation. **Ying Xiong:** Resources, Validation. **Yuanyuan Ma:** Resources. **Shi Yan:** Resources, Conceptualization. **Yue Yang:** Resources, Conceptualization. **Huabing Yin:** Visualization. **Xinxia Cai:** Funding acquisition, Project administration, Supervision.

Acknowledgements

This work is sponsored by the Key Research Programs (QYZDJ-SSW-SYS015) of Frontier Sciences, CAS, China; the National Key Research and Development Program (2017YFA0205902), China; the NSFC (61527815, 61771452 and 61775216), China.

Appendix A. Supplementary data

Supplementary data to this article can be found online at https://doi.org/10.1016/j.bios.2019.04.032.

References

Babamiri, B., Hallaj, R., Salimi, A., 2018. Biosens. Bioelectron. 99, 353–360.
Bast Jr, R.C., Klug, T.L., John, E.S., Jenison, E., Niloff, J.M., Lazarus, H., Berkowitz, R.S., Leavitt, T., Griffiths, C.T., Parker, L., 1983. N. Engl. J. Med. 309 (15), 883–887.
Dungchai, W., Chailapakul, O., Henry, C.S., 2009. Anal. Chem. 81 (14), 5821–5826.
Famulok, M., Mayer, G., Blind, M., 2000. Acc. Chem. Res. 33 (9), 591–599.
Fang, X., Tan, W., 2009. Acc. Chem. Res. 43 (1), 48–57.
Gao, W., Wang, W., Yao, S., Wu, S., Zhang, H., Zhang, J., Jing, F., Mao, H., Jin, Q., Cong, H., 2017. Anal. Chim. Acta 958, 77–84.
Ge, L., Wang, S., Song, X., Ge, S., Yu, J., 2012. Lab Chip 12 (17), 3150–3158.
Gordon, S.G., Cross, B.A., 1990. Cancer Res. 50 (19), 6229–6234.
Gubala, V., Harris, L.F., Ricco, A.J., Tan, M.X., Williams, D.E., 2011. Anal. Chem. 84 (2), 487–515.
Guo, S., Wang, E., 2007. Anal. Chim. Acta 598 (2), 181–192.
Hermann, T., Patel, D.J., 2000. Science 287 (5454), 820–825.
Jia, X., Liu, Z., Liu, N., Ma, Z., 2014. Biosens. Bioelectron. 53 (4), 160–166.
Lai, G., Yan, F., Ju, H., 2009. Anal. Chem. 81 (23), 9730–9736.
Lin, M.X., Lin, S.H., Li, Y.R., Chao, Y.H., Lin, C.H., Su, J.H., Lin, C.C., 2017. Mar. Drugs 15 (12), 378.
Lu, W., Lin, T., Wang, Y., Cao, X., Ge, J., Dong, J., Qian, W., 2015. Ionics 21 (4), 1141–1152.
Lv, H., Li, Y., Zhang, X., Gao, Z., Zhang, C., Zhang, S., Dong, Y., 2018. Biosens. Bioelectron. 112, 1–7.
Maehashi, K., Katsura, T., Kerman, K., Takamura, Y., Matsumoto, K., Tamiya, E., 2007. Anal. Chem. 79 (2), 782–787.
Martinez, A.W., Phillips, S.T., Butte, M.J., Whitesides, G.M., 2007. Angew. Chem. Int. Ed. 46 (8), 1318–1320.
Martinez, A.W., Phillips, S.T., Whitesides, G.M., Carrilho, E., 2009. ACS Publications.
Mazzu-Nascimento, T., Morbioli, G.G., Milan, L.A., Donofrio, F.C., Mestriner, C.A., Carrilho, E., 2017. Anal. Chim. Acta 950, 156–161.
Sanghavi, B.J., Wolfbeis, O.S., Hirsch, T., Swami, N.S., 2015. Microchim. Acta 182 (1–2), 1–41.
Sefah, K., Shangguan, D., Xiong, X., O'donoghue, M.B., Tan, W., 2010. Nat. Protoc. 5 (6), 1169.
Song, S., Wang, L., Li, J., Fan, C., Zhao, J., 2008. Trac. Trends Anal. Chem. 27 (2), 108–117.
Song, C., Yang, Y., Yang, B., Min, L., Wang, L., 2016. J. Mater. Chem. B. 4 (10), 1811–1817.
Sun, X., Ma, Z., 2013. Anal. Chim. Acta 780, 95–100.
Tsai, J.-Z., Chen, C.-J., Settu, K., Lin, Y.-F., Chen, C.-L., Liu, J.-T., 2016. Biosens. Bioelectron. 77, 1175–1182.
Wacker, R., Niemeyer, C.M., 2004. Chembiochem 5 (4), 453–459.
Wang, Y., Luo, J., Liu, J., Li, X., Kong, Z., Jin, H., Cai, X., 2018. Biosens. Bioelectron. 107, 47–53.
Wang, Y., Xu, H., Luo, J., Liu, J., Wang, L., Fan, Y., Yan, S., Yang, Y., Cai, X., 2016. Biosens. Bioelectron. 83, 319–326.
Wei, B., Mao, K., Liu, N., Zhang, M., Yang, Z., 2018. Biosens. Bioelectron. 121, 41–46.
Wu, L., Xiong, E., Zhang, X., Zhang, X., Chen, J., 2014. Nano Today 9 (2), 197–211.
Xu, Y., Zhang, X., Luan, C., Wang, H., Chen, B., Zhao, Y., 2017. Biosens. Bioelectron. 87, 264–270.
Yang, T., Gao, Y., Liu, Z., Xu, J., Lu, L., Yu, Y., 2017. Sensor. Actuator. B Chem. 239, 76–84.
Yu, S., Wei, Q., Du, B., Wu, D., Li, H., Yan, L., Ma, H., Zhang, Y., 2013. Biosens. Bioelectron. 48, 224–229.
Zhang, B., Zhang, X., Yan, H.H., Xu, S.J., Tang, D.H., Fu, W.L., 2008. Biosens. Bioelectron. 23 (1), 19–25.
Zhang, D., Li, W., Wang, H., Ma, Z., 2018. Sensor. Actuator. B Chem. 258, 141–147.
Zhao, C., Thuo, M.M., Liu, X., 2013. Sci. Technol. Adv. Mater. 14 (5), 054402.
Zhou, W., Huang, P.-J.J., Ding, J., Liu, J., 2014. Analyst 139 (11), 2627–2640.
Zong, C., Wu, J., Wang, C., Ju, H., Yan, F., 2012. Anal. Chem. 84 (5), 2410–2415.